Scaling of Skin-Friction Reduction Based on Plasma-Generated Streamwise Vortices

Xiaohui Wei and Yu Zhou

Abstract This work aims to investigate experimentally the dependence on the friction Reynolds number Re_τ of drag reduction (DR) in a turbulent boundary layer (TBL) using plasma-generated streamwise vortices (PGSV). The Re_τ examined is from 520 to 750. The developed actuator array produces three pairs of streamwise counter-rotating vortices in a fully developed TBL. The measured maximum spatially averaged drag reduction $DR_{\max}$ reaches 70% over the FE area (210 mm × 240 mm) at $Re_\tau = 520$. It has been found for the first time from the empirical scaling analysis of obtained experimental data that the DR scales with the strength of PGSV. which may have a profound impact upon engineering applications.

Keywords Boundary layer control · Drag reduction · Turbulent boundary layers

1 Introduction

Investigations on skin-friction drag reduction (DR) in the turbulent boundary layer (TBL) has been extensively pursued since the late 1970s due to its potential benefits in various engineering applications [1], particularly in aeronautics. DR can be passive and active. Active techniques may have a potential to change flow under control dramatically, thus attracting a great interest in the literature. One of the most popular active methods is to deploy the dielectric barrier discharge (DBD) plasma actuator (PA). Using this method, Cheng et al. [2] generated counter-rotating or co-rotating larger-scale streamwise vortices, achieving a maximum DR of 26% measured downstream of the PA array at the friction Reynolds number $Re_\tau = 572$ using a floating element (FE) force balance. The physical mechanism of DR was unveiled. However, being very small in wind tunnel experiments, the DR on the region where the PA array was placed could not be measured in their work. Furthermore, how the Reynolds

X. Wei · Y. Zhou (✉)
Center for Turbulence Control, Harbin Institute of Technology (Shenzhen), Shenzhen 518055, China
e-mail: yuzhou@hit.edu.cn

D. Kim et al. (eds.), *Fluid-Structure-Sound Interactions and Control*, Lecture Notes in Mechanical Engineering, https://doi.org/10.1007/978-981-97-6211-8_3

number may affect the control performance was not investigated wither. This study aims to address the two important issues.

2 Experimental Details

Experiments were performed in a closed-circuit wind tunnel at the Center for Turbulence Control, Harbin Institute of Technology (Shenzhen). The test section of the wind tunnel is 5.6 m long with a cross-section of 0.8 m × 1.0 m. The flow in the tunnel is generated through an axial fan driven by an electric motor, with a maximum power of 75 kW. The free-stream velocity U_∞ in the test section can be varied between 1.5 and 50 m/s, with a longitudinal turbulence intensity of less than 0.4% at $U_\infty = 2.4 \sim 5.0$ m/s where most of experiments are performed. A fully developed TBL with zero streamwise pressure gradient was generated over a smooth Perspex flat plate (4.8 m × 0.78 m) mounted in the test section. Two spanwise-aligned arrays of M4 screws were placed at 0.1 m downstream of the leading edge to trip the boundary layer. The streamwise pressure gradient is carefully adjusted through slightly inclining the flat plate to no more than 0.005 Pa/m. Most measurements are performed at 3.2 m downstream of the leading edge. The characteristic parameters of the TBL are given in Table 1 over $Re_\tau = 520 \sim 747$. The Re_τ range from 520 to 747 was selected, which corresponds to a U_∞ range of 2.4 to 5.0 m/s, for our study. This range was chosen because the power frequency of the wind tunnel is stable within these conditions. Additionally, this range was also used in Cheng et al. [2] to calibrate the FE force balance, making it convenient to compare our results with theirs. Furthermore, it is worth noting that the accuracy of the force balance may decrease when the U_∞ exceeds 10 m/s. Therefore, we selected this range to ensure the accuracy of our measurements.

The present PA (Fig. 1a) is the same as configuration B in Cheng et al. [2], though 0.2 mm-thick mica paper is used as the dielectric material to replace their Mylar and Kapton tapes. The lifespan of the new PA is greatly extended. As a result, it is possible to use the FE force balance to capture the real-time friction drag variation in the actuation area. The PA is placed on the FE (210 mm × 240 mm) of our newly improved force balance where the load cell is well isolated from the thermal and electrical effects associated with PA. This improved force balance is based on the

Table 1 Table captions should be placed above the tables

U_∞ (m/s)	δ (mm)	Re_τ	u_τ (m/s)	δ_ν (mm)
2.4	80	520	0.102	0.154
3.0	70	564	0.127	0.124
3.6	67	609	0.142	0.110
4.3	64	683	0.170	0.092
5.0	63	747	0.186	0.084

design of the balance used in Cheng et al. [2], and was found to have a measurement random error of less than 2.5% and a systematic error of less than 1%. To ensure the reliability of the experimental data, each measurement is repeated four times. A plasma-induced wall jet is generated from the upper to the lower electrode using a sinusoidal alternative current (AC) waveform applied with a peak-to-peak voltage $E_{p\text{-}p} = 1.2 \sim 6.0$ kV. The frequency of $E_{p\text{-}p}$ is fixed at 11 kHz. The discharge voltage waveform is measured using a capacitor voltage divider that is connected in parallel with the actuator. The voltage divider consists of two series-connected capacitors, C1 and C2, with a voltage ratio of $k_v = C2/(C1 + C2) = 1000$. As a result, the voltage at both ends of the larger capacitor C2 is approximately 1/1000 of the voltage on the actuator. The experimental power supply is connected to the two ends of the larger capacitor C2 in the capacitor voltage divider, and is applied with a peak-to-peak voltage of $E_{p\text{-}p}$. To measure the $E_{p\text{-}p}$, a 70 MHz RIGOL oscilloscope is used with a resolution of approximately 10 V, which is sufficient for the experimental voltage range.

3 Results and Scaling Law

The control performance is evaluated by the spatially averaged drag variation $\Delta F = (F_{on} - F_{off})/F_{off}$, where F_{on} and F_{off} are the measured skin friction forces on the FE with and without control, respectively. The ΔF depends on the $\underline{E_{p\text{-}p}}$ imposed as well as on Re_τ, as shown in Fig. 2a. In general, ΔF dips rapidly with increasing $\underline{E_{p\text{-}p}}$ for $Re_\tau = 520 \sim 747$, as noted by Cheng et al. [2] and Thomas et al. [3]. With increasing $\underline{E_{p\text{-}p}}$, the PGSVs and their associated spanwise wall jets are strengthened, resulting in a more pronounced DR. However, *DR* diminishes with increasing Re_τ, from 70% at $Re_\tau = 520$ to only 18% at $Re_\tau = 750$. This drop is attributed to the relatively weakened strength of PGSVs at higher Re_τ compared to their lower Re_τ counterparts.

Experimental data indicate that ΔF depends on three parameters, i.e. $\Delta F = f_1$ (Re_τ, $\overline{W}^+_{max}$, L^+), where $\overline{W}^+_{max}$ is the maximum plasma-induced spanwise wall-jet velocity measured at $y^+ = 17$ and L^+ is the distance between two positive electrodes in each actuator pair (superscript + denotes the wall unit). Based on Thomas et al. [3], careful analysis of experimental data along with numerous trial-and-error attempts unveils that the data of ΔF collapse well around one single curve once $\Gamma = [\log_{10}(k\,\overline{W}^+_{max})]/(L^+\delta^+)$ is used as the abscissa, where k is a constant related to the configuration of the PA and the power supply and δ^+ is the boundary layer disturbance thickness (Fig. 2b). That is, $\Delta F = f_1$ (Re_τ, $\overline{W}^+_{max}$, L^+) is now reduced to $\Delta F = f_2$ (Γ). Note that the Re_τ effect is embedded in $\overline{W}^+_{max}$, L^+ and δ^+ because the three parameters are all nondimensionalized by friction velocity u_τ or viscous length scale δ_ν that are directly related to Re_τ. To understand the scaling law $\Delta F = f_2$ (Γ) or the physical meaning of the scaling factor Γ, we introduce the boundary vorticity flux (BVF) $\boldsymbol{\sigma} = \nu \boldsymbol{n} \times (\nabla$

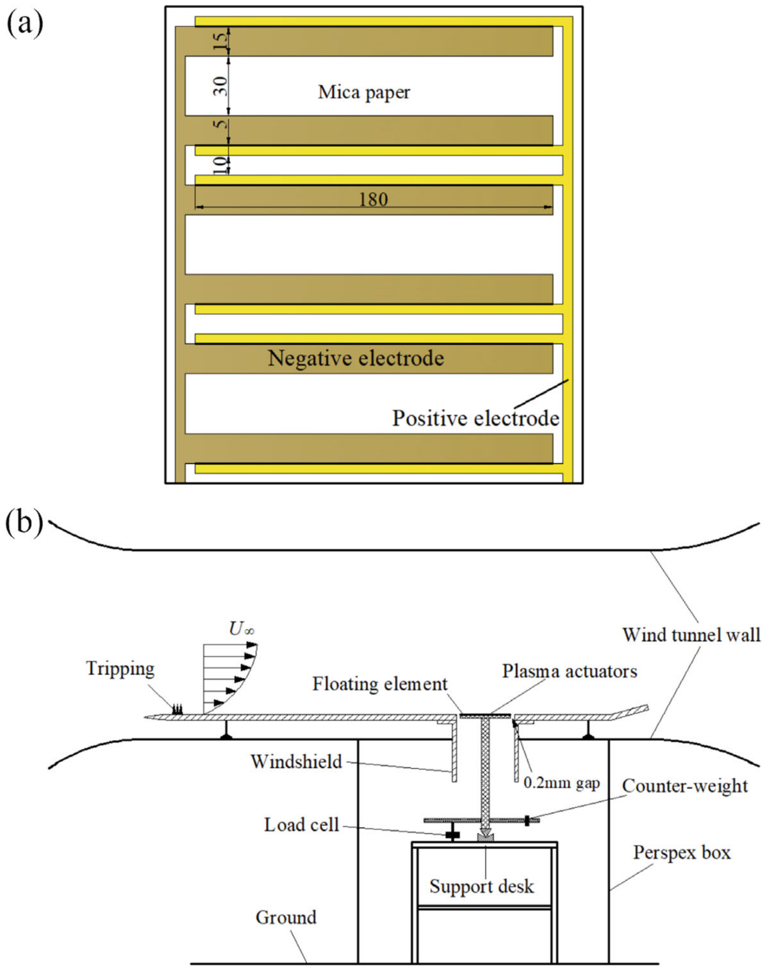

Fig. 1 **a** Schematic of the PA configuration (not to scale; dimensions in millimeters). **b** Schematic of experimental set-up for the generation of a turbulent boundary layer and the mounted floating-element force balance

$\times\ \boldsymbol{\omega}$) following Lyman [4] and Terrington et al. [5], where the vorticity vector $\boldsymbol{\omega} = [\omega_x, \omega_y, \omega_z] \approx [\omega_x, 0, 0]$, $\boldsymbol{n} = [1, 0, 0]$, ν is the kinetic viscosity of fluid, and ∇ is the differential operator. The ω_x is measured using particle image velocimetry (PIV). It is surprisingly found that Γ is in fact proportional to the strength of PGSV and is the sum of $|\boldsymbol{\sigma}|$ over an area where $|\omega_x| > 0.835|\omega_x|_{\max}$, i.e. $\Gamma = \sum|\boldsymbol{\sigma}|_{0.835} = \sum|\nu\boldsymbol{n} \times (\nabla \times \boldsymbol{\omega})|_{0.835}$. The equation clearly shows that Γ increases with $\boldsymbol{\omega}$ which represents the strength of the PGSV measured using PIV. Therefore, the results suggest that the DR scales with the strength of PGSV. Please refer to Fig. 2b.

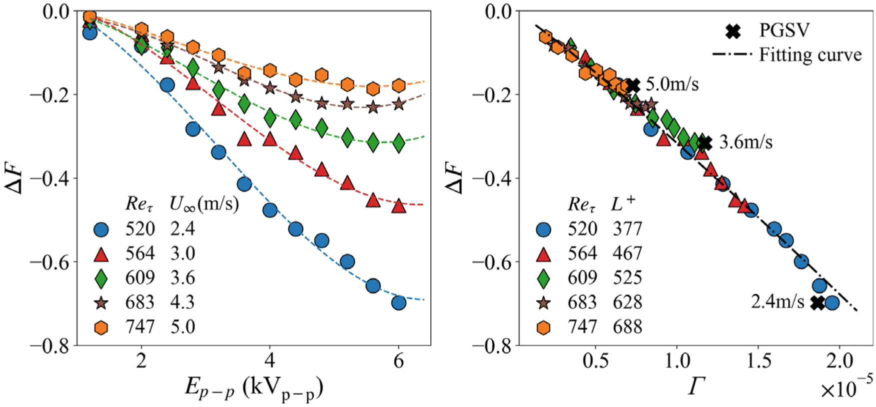

Fig. 2 **a** Dependence of the drag variation ΔF on the applied voltage on plasma actuators. **b** Dependence of the drag reduction ΔF on Γ. The blackbody cross symbols are determined by BVF $\boldsymbol{\sigma}$ when the all-applied voltages of the plasma actuator array are 6kV$_{\text{p-p}}$ at $U_\infty = 2.4$, 3.6 and 5.0 m/s

4 Conclusions

A TBL at $Re_\tau = 520 \sim 747$ is experimentally manipulated using a spanwise array of longitudinal PA with a view to reducing skin friction and investigating the scaling law for control parameters. Following conclusions can be drawn of out this work.

(1) A significant improvement has been made on our previously developed DBD plasma actuator, which prolongs greatly the lifespan of actuators. The dielectric material of PA is made of the 0.2 mm-thickness mica paper rather than Mylar and Kapton tapes, which may withstand a maximum voltage of 20 kV, instead of several kV, for a long time. Our high-resolution FE balance is also improved so that the load cell is well isolated from the thermal and electrical effects associated with PA. Thus, the PA can be placed on the FE to capture directly its averaged DR.

(2) A maximum DR of 70% is captured at $Re_\tau = 520$ in the region where the plasma actuators are placed. It is worth mentioning that Cheng et al. [2] measured a DR of 26% downstream of the PA array under similar experimental conditions. But *DR* diminishes with increasing Re_τ, dropping to 18% at $Re_\tau = 750$, which is ascribed to the weakened strength of PGSVs at higher Re_τ, as indicated in Fig. 2b.

(3) It has been found for the first time from empirical scaling analysis of obtained experimental data that $\Delta F = f_1\,(Re_\tau, \overset{-\,+}{W}_{\max}, L^+)$ can be reduced to $\Delta F = f_2\,(\Gamma)$. The BVF is introduced to interpret the scaling law or the physical meaning of the scaling factor Γ, which reveals that Γ is in fact proportional to the strength of the PGSV. Several interesting inferences can be made out of this scaling law. Firstly, *DR* increases approximately linearly with Γ i.e. $\Delta F = -\,10^{-5}\Gamma$. Secondly, given two of $\overset{-\,+}{W}_{\max}$, L^+ and δ^+, the effect of the remaining parameter

on ΔF may be determined from the scaling law. Thirdly, given Γ or ΔF, the required $\bar{W}^{+}_{max}$ that is related to the energy consumption of PA drops as the product of L^{+} and δ^{+} is reduced, that is, the control efficiency improves. Finally, ΔF can be predicted once Γ is known.

References

1. Kline S, Reynolds W, Schraub F, Runstadler P (1967) The structure of turbulent boundary layers. J Fluid Mech 30:741–773
2. Cheng XQ, Wong CW, Hussain F, Schroder W, Zhou Y (2021) Flat plate drag reduction using plasma-generated streamwise vortices. J Fluid Mech 918:A24
3. Thomas FO, Corke TC, Duong A et al (2019) Turbulent drag reduction using pulsed-DC plasma actuation. J Phys D Appl Phys 52:434001
4. Lyman FA (1990) Vorticity production at a solid boundary. Appl Mech Rev 43:157–157
5. Terrington S, Hourigan K, Thompson M (2022) Vorticity generation and conservation on generalised interfaces in three-dimensional flows. J Fluid Mech 936:A44